

Learning Functional Transduction

Mathieu Chalvidal^{1 2 3} Thomas Serre^{1 2} Rufin VanRullen^{1 3}

Abstract

Research in Machine Learning has polarized into two general regression approaches: Transductive methods derive estimates directly from available data but are usually problem unspecific. Inductive methods can be much more particular, but generally require tuning and compute-intensive searches for solutions. In this work, we adopt a hybrid approach: We leverage the theory of Reproducing Kernel Banach Spaces (RKBS) and show that transductive principles can be induced through gradient descent to form efficient *in-context* neural approximators. We apply this approach to RKBS of function-valued operators and show that once trained, our *Transducer* model can capture on-the-fly relationships between infinite-dimensional input and output functions, given a few example pairs, and return new function estimates. We demonstrate the benefit of our transductive approach to model complex physical systems influenced by varying external factors with little data at a fraction of the usual deep learning training computation cost for partial differential equations and climate modeling applications.

In statistical learning, transduction refers to the process of reasoning directly from observed (training) cases to new (test) cases, and contrasts with induction, which amounts to extracting general rules from observed training cases. Vapnik (2006) condensed this philosophy into an imperative principle for statistical learning: “*When solving a problem of interest, do not solve a more general problem as an intermediate step. Try to get the answer that you really need but not a more general one.*”. Transductive machine learning has yielded some of the most useful regression algorithms, from K -nearest neighbors (Cover & Hart, 1967) to support vector machines (Boser et al., 1992) or Gaussian processes

¹Artificial and Natural Intelligence Toulouse Institute, Université de Toulouse, France ²Carney Institute for Brain Science, Dpt. of Cognitive Linguistic & Psychological Sciences, Brown University, Providence, RI 02912 ³Centre de Recherche Cerveau & Cognition CNRS, Université de Toulouse. Correspondence to: M. Chalvidal <mathieu_chalvid@brown.edu>.

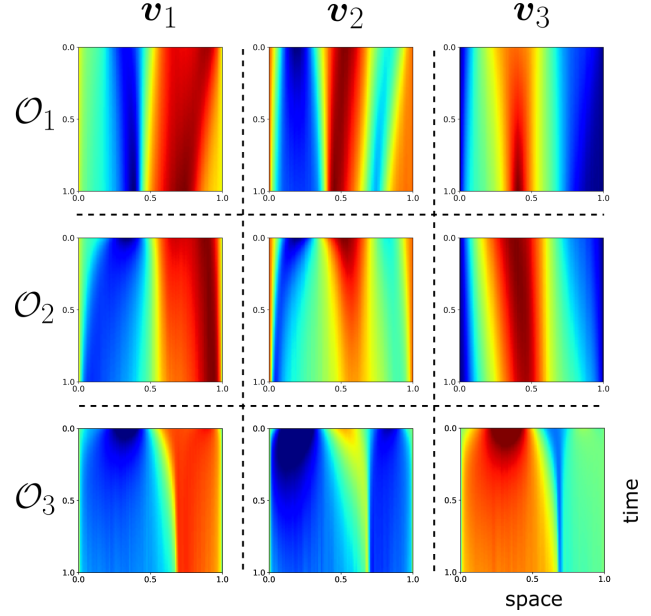


Figure 1. Examples of image functions $u = \mathcal{O}(v)$ for different functional operators ($\mathcal{O}_1, \mathcal{O}_2, \mathcal{O}_3$) and different inputs (v_1, v_2, v_3) obtained with the same neural *Transducer* conditioned with different relevant examples pairs $(v, \mathcal{O}_i(v))_{i \leq 3}$. Each operator corresponds to a one-dimensional advection-diffusion-reaction equation on the domain $(x, t) \in [0, 1]^2$ with randomly sampled functional parameters unseen during training. Our model is trained on predicting the functional solution at $t = 1$ but extrapolates to all intermediate solutions along the temporal dimension.

(Williams & Rasmussen, 1995). A major advantage of such systems is their wide applicability and the straightforward construction of estimates. Research in deep learning, however, has mostly endeavored to find inductive solutions by crafting networks that generalize from large datasets, relying on the empirical evidence that stochastic gradient descent is a powerful control rule faithfully encoding functional relationships between input and outputs into the network weights. Nevertheless, this paradigm has shown limits: Gradient-based training is compute-intensive and requires a large amount of data to approximate a single functional map. This may be particularly problematic for real-world applications where data has heterogeneous sources or only a few examples of the relationship of interest are available. Moreover, these solutions generalize poorly outside of the training distribution (Jin et al., 2020), and a slight modifica-

tion of the target function might require expensive retraining as well as forgetting of the previous solution (McCloskey & Cohen, 1989). Finally, they show poor robustness to adversarial attack (Szegedy et al., 2013) or anomalous data contamination of the training distribution (Zhang et al., 2021). Ultimately, to become practically useful, such data-driven methods should also perform well outside of the data set they are trained with and they should be able to extrapolate to different parameters and contexts. Still, deep learning systems capable of flexibly and robustly adapting their response to small data regimes are yet to come.

In this work, we explore a hybrid solution to tackle functional regression problems defined in Banach spaces by meta-learning a deep transductive regression model that can produce relevant estimates given original datasets. This meta-problem represents itself as an infinite-dimensional regression problem, which consists in finding a program associating a target function to its corresponding exemplar dataset. We leverage the theory of Reproducing Kernel Banach Spaces (RKBS) (Zhang, 2013; Lin et al., 2022) and interpret the recent attention mechanism of the Transformer (Vaswani et al., 2017) as a parametric form of a reproducing kernel that we use to build functional approximators in various RKBS. Our framework allows us to handle both RKBS defined between finite and infinite-dimensional spaces, allowing us to manipulate functional data, and performing operator regression given a few examples of input-output pairs. While kernel regression is usually plagued with the “curse of dimensionality” (Bellman, 1966; Aggarwal et al., 2001), we show that our approach escapes this pitfall and manages to learn well-adapted operator-valued RKBS kernels. From a control perspective, our method can be interpreted as building an *open-loop controller* where input-output examples condition a neural operator to produce a desired functional response. From a machine learning perspective, our method can be interpreted as a form of *in-context* learning in infinite-dimensional function spaces.

Contributions

- We introduce a deep kernel method for operator regression, by meta-learning to attend to collections of input-output functions in order to learn to approximate a functional mapping. To the best of our knowledge, our proposal is the first to marry infinite dimensional RKBS with deep networks, which opens up new applications for transductive functional regression.
- We demonstrate the flexibility and efficiency of our framework for fitting function-valued operators and show that our model can generalize to new operator instances in two PDEs regression and climate modeling problems.

The remainder of the paper is organized as follows: in Sec-

tion 1 we discuss previous related work. In Section 2 we introduce the mathematical formulation of the functional transductive regression problem and describe more formally our model in section 4. We report in section 5 experimental results in different settings. Finally, in Section 6 we summarise our work and outline future research directions.

1. Related work

Transductive Machine learning – The idea of determining statistical predictions directly from exemplar data has been more formally described in Gammernan et al. (1998); Vapnik (1999) with pervasive applications in Machine Learning: Estimators relying on relational structures between data points such as K -nearest neighbors (Cover & Hart, 1967) and kernels methods (Nadaraya, 1964; Watson, 1964) build regression estimates by weighting examples with respect to a certain metric space. Further, the “kernel trick” allows to embed possibly infinite-dimensional features (Ferraty & Vieu, 2006) into finite Gram matrix representations that are also well-suited for multi-task regression (Evgeniou et al., 2005; Caponnetto et al., 2008). Gaussian processes (Williams & Rasmussen, 1995) combine transduction with Bayesian modeling to regress a posterior distribution over possible functions. However, these techniques might suffer from the so-called “curse of dimensionality”: with growing problem dimensionality, the density of the exemplar point diminishes, which increases their statistical variance. More recent work combining deep learning with transductive inference has shown promising results for few-shot learning even in high-dimensional spaces (Snell et al., 2017b) or for sequence modeling (Jaitly et al., 2015), but the vast majority of neural networks still remain purely inductive. Finally, modern Hopfield networks (Ramsauer et al., 2020) have been shown to implement various dynamic operations on sets of representations related to the Transformer attention, offering the possibility to leverage transductive computation in the deep learning realm.

Neural operator learning – While regression with neural networks has primarily been applied to learning mappings between finite-dimensional spaces, their impressive approximation abilities have been generalized to operator mappings between function spaces. Chen & Chen (1995) showed that finite neural parametrization can approximate well infinite-dimensional functional relationships. More recent work on neural operator regression has shown promising results (Lu et al., 2019), especially when mixed with tools from functional analysis and physics (Raissi et al., 2017; Li et al., 2020a; Gupta et al., 2021; Li et al., 2020b; Nelsen & Stuart, 2021; Wang et al., 2021; Roberts et al., 2021) and constitutes a booming research direction in particular for physical applications (Goswami et al., 2022; Pathak et al., 2022; Vinuesa & Brunton, 2022; Wen et al., 2022; Pickering

et al., 2022). Such systems are able to approximate infinite-dimensional functional objects in a highly compressed form, and potentially offer a much more powerful substrate for learning and manipulating representations than static vectors. Orthogonally, while the recent ground-breaking attentional computation of the Transformer was interpreted as a Petrov-Galerkin projection (Cao, 2021) or through Reproducing Kernel Hilbert Space theory (Kissas et al., 2022) for building neural operators, these perspectives propose to apply attention to fit a single target operator. We will show the theory of reproducing kernel Banach space suggests that we can take further advantage of kernel modeling together with neural operators in order to flexibly solve infinitely many operator regression problems.

Meta-learning and in-context learning – Research for improving deep learning training has accelerated in recent years. Promising work has regarded this problem from the perspective of "learning to learn" or meta-learning (Schmidhuber et al., 1997; Vilalta & Drissi, 2002), by either explicitly treating a gradient descent sequence as an optimizable object (Finn et al., 2017) or modeling an optimizer as a black-box autoregressive model (Santoro et al., 2016; Ravi & Larochelle, 2017). Another orthogonal approach aims at learning a generalizing metric that allows for straightforward object class regression in a latent space (Snell et al., 2017a; Sung et al., 2018). More recently, converging findings in various domains from reinforcement learning (Mishra et al., 2018; Laskin et al.), natural language processing (Brown et al., 2020; Xie et al., 2021; Olsson et al., 2022) and functional regression (Garg et al., 2022) have established the ability of set-based attentional computation in the Transformer (Vaswani et al., 2017) for *in-context* learning, by flexibly extracting functional relationships and performing dynamic association such as linguistic analogy or few-shot behavioral imitation. We show that the theory of RKBS can help interpret such property and extends it to function-valued operators regression.

2. Problem formulation

2.1. Notations

Let $(\mathcal{V}, \mathfrak{A}, \mu)$ be a σ -finite measure space referred as the input space and $(\mathcal{U}, \|\cdot\|_{\mathcal{U}})$ a Banach space referred as the output space. We consider \mathcal{B} , the Bochner space of strongly μ -measurable functions $\mathcal{O} : \mathcal{V} \mapsto \mathcal{U}$. We note that \mathcal{B} is a Banach space with the norm $\|\cdot\|_{\mathcal{B}} = (\int \|\cdot\|_{\mathcal{U}} d\mu)$. Throughout, we assume that all considered Banach spaces \mathcal{S} are uniformly convex and uniformly Fréchet-differentiable, which allows us to equip them with their compatible semi-inner product $\langle \cdot, \cdot \rangle_{\mathcal{S}} : \mathcal{S} \times \mathcal{S} \mapsto \mathbb{C}$, and to define their bijective dual space $\mathcal{S}^* := \{s' \mapsto \langle s', s \rangle_{\mathcal{S}}, s \in \mathcal{S}\}$ (Giles, 1967; Koehler, 1971). We also note $\mathcal{L}(\mathcal{U}, \mathcal{B})$ (resp. $\mathcal{L}(\mathcal{U})$) the set of bounded linear operators from \mathcal{U} to \mathcal{B} (resp. to itself).

2.2. The meta-regression problem

We consider the problem of building a computationally tractable regression map \mathcal{T} able to approximate any element $\mathcal{O} \in \mathcal{B}$ from a "representative" finite collection of example pairs $\mathcal{E}_{\mathcal{O}} = \{(v_i, u_i) \mid v_i \sim \mu, u_i = \mathcal{O}(v_i)\}_{i \leq I}$ with $I \in \mathbb{N}$. Given an error level $\epsilon \in \mathbb{R}$, we would like \mathcal{T} to verify for all $\mathcal{O}, \mathcal{E}_{\mathcal{O}}$:

$$\int_{\mathcal{V}} \|\mathcal{T}(\mathcal{E}_{\mathcal{O}})(v) - \mathcal{O}(v)\|_{\mathcal{U}} d\mu(v) < \epsilon \quad (1)$$

Finding efficient methods for identifying and modeling elements $\mathcal{O} \in \mathcal{B}$ is a pervasive but complex meta-regression problem. Gradient-based optimization of neural networks have shown generic and powerful regression properties. Fundamentally, these techniques work by induction: They rely on a stochastic optimization process of a predefined criterion function to capture statistical regularities of a single map \mathcal{O} into a parametric neural mapping \mathcal{T}_{θ} . After training, data $\mathcal{E}_{\mathcal{O}}$ is discarded for inference, assuming sufficient inductive alignment of \mathcal{T}_{θ} with \mathcal{O} , i.e. $\forall v \in \mathcal{V}, \mathcal{T}_{\theta}(v) \approx \mathcal{O}(v)$. Examples of such regression techniques with neural networks are PINNs (Raissi et al., 2019) for finite-dimensional spaces, and DeepOnet (Lu et al., 2019) or FNO (Li et al., 2020a) in the infinite-dimensional case of operator regression. Despite its theoretical ubiquity, such an approach is plagued with multiple problems discussed above: heavy training procedure with high sample complexity, weak robustness and adaptability to out-of-distribution samples. Here instead, we propose to adopt a meta-learning perspective by leveraging the theory of reproducing kernel Banach spaces combined with the universal approximation abilities of deep networks to learn the regression program itself.

3. Reproducing Kernel Banach Space regression

We start by recalling some elements of the theory of Reproducing Kernel Banach Spaces (RKBS) developed in Zhang (2013), which will be useful to build our neural kernel regression model. For a more in-depth treatment of RKBS, see also Lin et al. (2022).

Theorem 1 (Vector-valued RKBS) *A \mathcal{U} -valued reproducing kernel Banach space \mathcal{B} of operators from \mathcal{V} to \mathcal{U} is a Banach space such that for all $v \in \mathcal{V}$, the point evaluation $\delta_v : \mathcal{B} \mapsto \mathcal{U}$ defined as $\delta_v(\mathcal{O}) = \mathcal{O}(v)$ is continuous. In this case, there exists a unique function $\mathcal{K} : \mathcal{V} \times \mathcal{V} \mapsto \mathcal{L}(\mathcal{U})$ such that for all $(v, u) \in \mathcal{V} \times \mathcal{U}$:*

$$\begin{cases} v' \mapsto \mathcal{K}(v, v')(u) \in \mathcal{B} \\ \forall \mathcal{O} \in \mathcal{B}, \langle \mathcal{O}(v), u \rangle_{\mathcal{U}} = \langle \mathcal{O}, \mathcal{K}(v, \cdot)(u) \rangle_{\mathcal{B}} \\ \forall v' \in \mathcal{V}, \|\mathcal{K}(v, v')\|_{\mathcal{L}(\mathcal{U})} \leq \|\delta_v\|_{\mathcal{L}(\mathcal{B}, \mathcal{U})} \|\delta_{v'}\|_{\mathcal{L}(\mathcal{B}, \mathcal{U})} \end{cases} \quad (2)$$

Informally, definition (2) states that the image of *any* function \mathcal{O} of \mathcal{B} at a given point \mathbf{v} can be expressed in terms of a single function \mathcal{K} . The latter is hence called the *reproducing kernel* of \mathcal{B} and our goal is to leverage the unicity of \mathcal{K} to form a single approximator for all operators in \mathcal{B} . However, the previous theorem does not provide explicit information on how to construct such function \mathcal{K} . Fortunately, the feature maps characterization of RKBS will give us a structure to build \mathcal{K} . We first define for any linear operator $T \in \mathcal{L}(\mathcal{S}_1, \mathcal{S}_2)$ between two Banach spaces $\mathcal{S}_1, \mathcal{S}_2$, the generalized adjoint $T^\dagger \in \mathcal{L}(\mathcal{S}_2, \mathcal{S}_1)$ as the application verifying $\langle Ts, s' \rangle_{\mathcal{S}_1} = \langle s, T^\dagger s' \rangle_{\mathcal{S}_2}$ for all $(s, s') \in \mathcal{S}_1 \times \mathcal{S}_2$.

Theorem 2 (Feature map characterization of RKBS) *A function $\mathcal{K} : \mathcal{V} \times \mathcal{V} \mapsto \mathcal{L}(\mathcal{U})$ is the reproducing kernel of some \mathcal{U} -valued RKBS if and only if there exist a Banach space \mathcal{B} and a mapping $\Phi : \mathcal{V} \mapsto \mathcal{L}(\mathcal{B}, \mathcal{U})$ such that:*

$$\begin{cases} \forall (\mathbf{v}, \mathbf{v}') \in \mathcal{V}^2, \mathcal{K}(\mathbf{v}, \mathbf{v}') = \Phi(\mathbf{v}')(\Phi^\dagger(\mathbf{v})) \\ \overline{\text{span}}\{(\Phi(\mathbf{v})^\dagger(\mathbf{u}))^*, \mathbf{v} \in \mathcal{V}, \mathbf{u} \in \mathcal{U}\} = \mathcal{B}^* \end{cases} \quad (3)$$

with $\Phi^\dagger : \mathcal{V} \mapsto \mathcal{L}(\mathcal{U}, \mathcal{B})$ defined by: $\forall \mathbf{v}, \Phi^\dagger(\mathbf{v}) = (\Phi(\mathbf{v}))^\dagger$.

Theorem (2) reformulates the kernel construction problem into a search for its corresponding feature maps Φ and Φ^\dagger (in RKBS, contrary to RKHS, the adjoint can generally not be directly expressed from the operator itself due to the non-additivity of the semi-inner product), for which we can find parametric approximations. It also constitutes a generalisation of the Transformer attention mechanism. To see this, let us assume that \mathcal{V} and \mathcal{U} are finite-dimensional and define $W_\theta \in \mathcal{L}(\mathbb{R}^p, \mathcal{U})$, $(Q_\theta, K_\theta) \in \mathcal{L}(\mathcal{V}, \mathbb{R}^p)^2$, $V_\theta \in \mathcal{L}(\mathcal{U}, \mathbb{R}^p)$ and σ a softmax normalization. Forming the following parametric kernel κ_θ ;

$$\kappa_\theta(\mathbf{v}, \mathbf{v}')(\mathbf{u}) \triangleq W_\theta \left(\sigma(Q_\theta(\mathbf{v}').(K_\theta(\mathbf{v}))^T) \cdot V_\theta(\mathbf{u}) \right) \quad (4)$$

we see that (4) corresponds to the Transformer key-query attention as well as a particular kernel construction following Theorem (2). We will use (4) to build our kernel, but note that other constructions are possible. Finally, in order to apply the kernel representation to available data $\mathcal{E}_\mathcal{O}$ for approximating a specific operator \mathcal{O} , we present an extension of the representer theorem to vector-valued RKBS:

Theorem 3 (RKBS Representer Theorem) *Let \mathcal{B} be a operator-valued RKBS from \mathcal{V} to \mathcal{U} . Then the minimal norm interpolation problem:*

$$\inf_{\mathcal{O} \in \mathcal{B}} \{\|\mathcal{O}\|_{\mathcal{B}}, \text{ s.t. } \mathcal{O}(\mathbf{v}_i) = \mathbf{u}_i, i \leq I\} \quad (5)$$

admits a unique minimizer \mathcal{O}_0 . Moreover, \mathcal{O}_0 is the solution of (5) if and only if $\mathcal{O}_0(\mathbf{v}_i) = \mathbf{u}_i$ for all $i \leq I$ and $\mathcal{O}_0^ \in \overline{\text{span}}\{\mathcal{K}(\mathbf{v}_i, \cdot)(\mathbf{u})^*, i \leq I, \mathbf{u} \in \mathcal{U}\}$.*

The representer theorem tells us that there exists $(\mathbf{y}_i)_{i \leq I}$ functions in \mathcal{U} such that $\mathcal{O}_0^* = \sum_{i \leq I} (\mathcal{K}(\mathbf{v}_i, \cdot)(\mathbf{y}_i))^*$. Here, contrary to reproducing kernel Hilbert space theory, we cannot directly solve an explicit linear problem in $(\mathbf{y}_i)_{i \leq I}$ to find the minimizer of (5). Instead, we show in the next section that we can jointly learn the kernel \mathcal{K}_θ together with a deep network mapping $(\mathbf{u}_i = \mathcal{O}(\mathbf{v}_i))_{i \leq I}$ to $(\tilde{\mathbf{y}}_i)_{i \leq I}$ such that $\mathcal{O}_0(\mathbf{v}) = \sum_{i \leq I} \mathcal{K}_\theta(\mathbf{v}_i, \mathbf{v})(\tilde{\mathbf{y}}_i)$.

4. Proposed approach: The Transducer model

4.1. Discretization

We now focus for the rest of the paper on the case of infinite-dimensional functional input and output spaces \mathcal{V} and \mathcal{U} . In this case, for numerical computation purpose, we can accommodate different types of function representations previously proposed for neural operator regression and allowing for evaluation at an arbitrary point of the domain. For instance, output function representations can be defined as a linear combination of learned or hardcoded finite set of functions, as in Lu et al. (2019); Bhattacharya et al. (2020). We focus instead on a different approach inspired by Fourier Neural Operators (Li et al., 2020a), by applying our model on the M first modes of the Fourier transform of functions $(\mathbf{v}_i, \mathbf{u}_i)_{i \leq I}$, and transform back its output, allowing us to work with discrete and finite function representations.

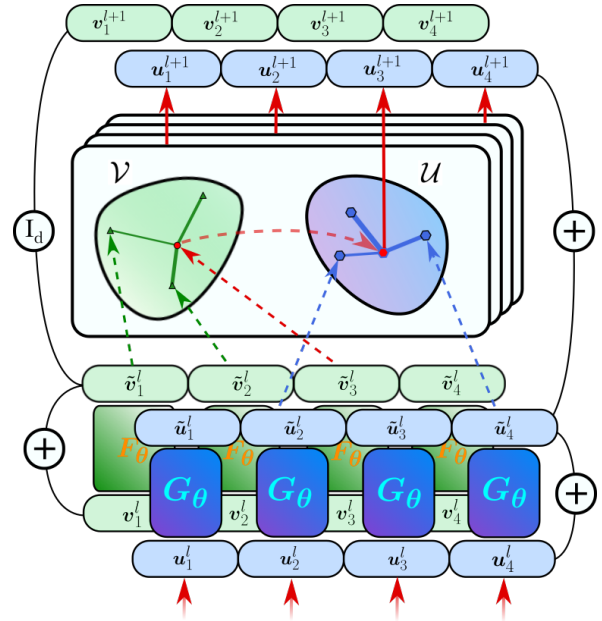


Figure 2. Schema of a Transducer layer. A collection of input and output elements $(\mathbf{v}_i^l, \mathbf{u}_i^l)$ are transformed in parallel by one-layer fully connected residual networks into intermediate representations $(\tilde{\mathbf{v}}_i^l, \tilde{\mathbf{u}}_i^l)$. Every element $(\tilde{\mathbf{u}}_i^l)$ is further transformed by the kernel operation \mathcal{K}_{θ_i} which extract relations between $(\tilde{\mathbf{v}}_i^l)$ to form the residual contribution $\sum_i \kappa_\theta(\tilde{\mathbf{v}}_i^l, \tilde{\mathbf{v}}_j^l)(\tilde{\mathbf{u}}_i^l)$.

Our kernel model consists in a deep neural network of depth L building a sequence of representations $(\mathbf{v}_i^\ell, \mathbf{u}_i^\ell)_{i \leq I, \ell \leq L}$ starting with $(\mathbf{v}_i^1, \mathbf{u}_i^1)_{i \leq I} = \mathcal{E}_\mathcal{O}$ and defined by the following iteration:

$$\begin{cases} \mathbf{v}_i^{\ell+1} = \mathbf{v}_i^\ell + F_\theta^\ell(\mathbf{v}_i^\ell) \\ \mathbf{u}_i^{\ell+1} = \mathbf{u}_i^\ell + G_\theta^\ell(\mathbf{u}_i^\ell) + \mathcal{T}_\theta^\ell(\mathbf{v}_i^\ell + F_\theta^\ell(\mathbf{v}_i^\ell)) \end{cases} \quad (6)$$

where F_θ^ℓ (resp. G_θ^ℓ) corresponds to pointwise feedforward networks transformations applied in parallel to representations $(\mathbf{v}_i^\ell)_{i \leq I}$ (resp. $(\mathbf{u}_i^\ell)_{i \leq I}$) and $\mathcal{T}_\theta^\ell : \mathcal{V} \mapsto \mathcal{U}$ are intermediate kernel transformations :

$$\forall \mathbf{v} \in \mathcal{V}, \quad \mathcal{T}_\theta^\ell(\mathbf{v}) = \sum_{i \leq I} \kappa_\theta^\ell(\tilde{\mathbf{v}}_i^\ell, \mathbf{v})(\tilde{\mathbf{u}}_i^\ell) \quad (7)$$

where $(\tilde{\mathbf{v}}_i^\ell, \tilde{\mathbf{u}}_i^\ell)_{i \leq I}$ refers to the residual transformations $(F_\theta^\ell(\mathbf{v}_i^\ell) + \mathbf{v}_i^\ell, G_\theta^\ell(\mathbf{u}_i^\ell) + \mathbf{u}_i^\ell)_{i \leq I}$. Note that equations (6) and (7) allows to handle various set sizes. We refer to our system as a *Transducer*, both as a tribute to the Transformer (Vaswani et al., 2017) computation mechanism from which it is derived and by analogy with engineering devices that convert a signal from one form to another. Our intuition is that network depth allows for a better kernel approximation by iteratively refining the operator estimate and approximate on-the-fly the solution functions $(\tilde{\mathbf{y}}_i)_{i \leq I}$. We investigate further the influence of network depth and its parameterization in the experimental section, noting for instance that sharing the non-linear transformations (F^ℓ, G^ℓ) for the input and output domains can be beneficial to regression performance. Finally, the operator image estimate of any $\mathbf{v} \in \mathcal{V}$ corresponds to the sum of residual transformations:

$$\hat{\mathcal{O}}(\mathbf{v}) = \mathcal{T}_\theta(\mathbf{v}|\mathcal{E}_\mathcal{O}) = \sum_{\ell \leq L} \sum_{i \leq I} \kappa_\theta^\ell(\tilde{\mathbf{v}}_i^\ell, \mathbf{v})(\tilde{\mathbf{u}}_i^\ell) \quad (8)$$

where the sequence (\mathbf{v}^ℓ) is constructed in the same way as $(\mathbf{v}_i^\ell)_{i \leq I}$ starting with $\mathbf{v}^1 = \mathbf{v}$. Note that the model allows for jointly building sequence (\mathbf{v}^ℓ) with $(\mathbf{v}_i^\ell)_{i \leq I}$, as well as for batch inference by simply masking the corresponding cross-relational features during the kernel operations. Further, all those operations correspond to parallelizable tensorial GPU-accelerated operations such that regression estimates are produced orders of magnitude faster than gradient-based regression methods.

4.2. Training

Our goal is to learn the sequence of kernel operations $(\kappa_\theta^\ell)_{\ell \leq L}$ as well as $(F_\theta^\ell, G_\theta^\ell)_{\ell \leq L}$ in order to approximate solutions of (5). Let us assume that elements \mathcal{O} are sampled according to a probability measure β , and that for each \mathcal{O} , $\mathcal{E}_\mathcal{O}$ is sampled according to a probability measure $\gamma_\mathcal{O}$ from the set of possible example sets with finite cardinality $E_\mathcal{O}$. Our meta-learning objective can be defined as:

$$\mathcal{J}(\theta) = \mathbb{E}_{\mathcal{O} \sim \beta} \left[\mathbb{E}_{\mathcal{E}_\mathcal{O} \sim \gamma_\mathcal{O}} \left[\|\mathcal{T}_\theta^L(\cdot|\mathcal{E}_\mathcal{O}) - \mathcal{O}\|_\mathcal{B} \right] \right] \quad (9)$$

that can be tackled with gradient-based optimization given that \mathcal{T}_θ^L is differentiable w.r.t parameters θ . In order to estimate gradient of (9), we form the empirical Monte-Carlo estimator over a batch of N operators \mathcal{O} and J query function \mathbf{v}_j :

$$\nabla_\theta \mathcal{J}(\theta) \approx \frac{1}{NJ} \sum_{n \leq N} \sum_{j \leq J} \nabla_\theta \|\mathcal{T}_\theta(\mathbf{v}_j|\mathcal{E}_{\mathcal{O}_n}) - \mathbf{u}_j^n\|_\mathcal{U} \quad (10)$$

with $\mathbf{u}_j^n = \mathcal{O}_n(\mathbf{v}_j)$. In practice, using a single operator ($N=1$) to estimate (10) works well and training is very stable, mitigating the linearly increasing cost of storing the I examples pairs in memory. We show empirically that such meta-optimized models are able to efficiently approximate diverse sets of operators \mathcal{O} given small amounts of data in a single feedforward pass, bypassing the need for gradient-based tuning. This ability can greatly improve neural-based operators applicability since real physical systems data is often scarce and canonical training approaches require large amounts of it. Furthermore, to the best of our knowledge, this work is the first to show that neural networks can learn transductive regression programs on space of operators.

5. Experiments

In this section, we show that our model can perform online regression of various operators defined on scalar and vector-valued function spaces arising in physical science.

Training details – We construct our network by merely stacking Transducer layers defined as above with one-layer perceptrons with layer normalization (Ba et al., 2016) and GeLU activation functions (Hendrycks & Gimpel, 2016) for (F^ℓ, G^ℓ) and followed by the kernel operation. We carry out meta-learning of operator regression in the following way: We gather a meta-dataset of N_{train} operators example sets $\mathcal{E}_{\mathcal{O}_n}$ with i example function pairs. At each training step, we randomly sample a set $\mathcal{E}_{\mathcal{O}_n}$ as well as query subset \mathcal{Q} of output functions $(\mathcal{O}(\mathbf{v}_i))_{i \in \mathcal{Q}}$ to be estimated. We form the input $\tilde{\mathcal{E}}_{\mathcal{O}_n}$ by concatenating pairs of a non-overlapping set \mathcal{I} of example elements $(\mathbf{v}_i, \mathbf{u}_i)_{i \in \mathcal{I}}$ with pairs of the query set $(\mathbf{v}_i, \mathbf{u}_i)_{i \in \mathcal{Q}}$ with output elements $(\mathbf{u}_i)_{i \in \mathcal{Q}}$ set to zero. We train our model to minimize the sum of L_2 error between each output function of the set \mathcal{Q} and its corresponding ground truth $\mathbf{u}(x) = \mathcal{O}_n(\mathbf{v})(x) = s(x, 1)$. We use the Adam optimizer (Kingma & Ba, 2014) to train for a fixed number of steps with an initial learning rate of $2e-4$ that is gradually halved along the training. All the computation is carried on a single Nvidia Titan Xp GPU with 12GB memory. Further details on data generation and baseline settings are given in SI.

5.1. Regression of Advection-Diffusion Reaction PDEs

First, we examine the problem of regressing operators \mathcal{O} associating functions \mathbf{v} from $\mathcal{V} \subset C([0, 1], \mathbb{R})$ to their fu-

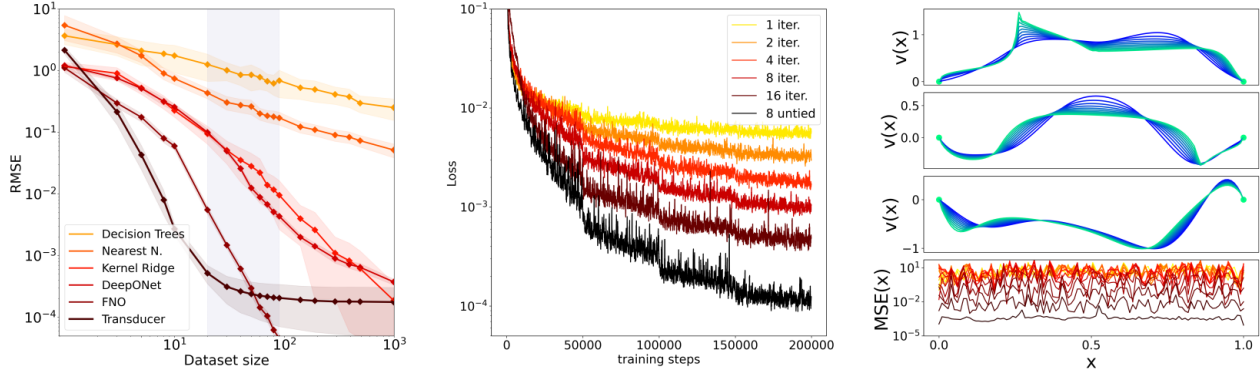


Figure 3. Left: Mean relative MSE with a confidence interval at 90% on unseen operators as a function of the dataset size for each regression method. The grey area corresponds to dataset cardinalities seen during training for the *Transducer*. All other methods are trained from scratch with a corresponding number of original examples. **Middle:** Evolution of the training loss of *Transducers* with different number of kernel transformations. Allowing more iterations of kernel transformation improves performance, with untied weights yielding the best performance. **Right:** Up - 3 examples of the evolution of the state $s(x, t)$ as a function of spatial dimension for different ADR equations $E(\delta, \nu, k)$. Bottom - Evolution of the MSE of intermediate representations (u^ℓ) colored by iteration number. The decreasing profile along with the performance trend observed with a growing number of iterations suggest network depth allows the model to progressively refine its function estimate.

ture solution $u = \mathcal{O}(v) \subset C([0, 1], \mathbb{R})$ with respect to advection-diffusion-reaction equations defined on the domain $\Omega = [0, 1] \times [0, t]$ with Dirichlet boundary conditions $s(0, t) = s(1, t) = 0$. We consider the space \mathcal{B} of operators $\mathcal{O}_{(\delta, \nu, k, t)}$ specifically defined by the 4-uplet (δ, ν, k, t) , such that $v(x) = s(x, 0)$, $u(x) = s(x, t)$ and s follows equation $E(\delta, \nu, k)$ that depends on unknown random continuous spatially-varying diffusion $\delta(x)$, advection $\nu(x)$, and a scalar reaction term $k \sim \mathcal{U}[0, 0.1]$.

$$\begin{aligned} \partial_t s(x, t) = & \underbrace{\nabla \cdot (\delta(x) \nabla_x s(x, t))}_{\text{diffusion}} + \underbrace{\nu(x) \nabla_x s(x, t)}_{\text{advection}} \\ & + \underbrace{k \cdot (s(x, t))^2}_{\text{reaction}} \end{aligned} \quad (11)$$

Eq. (11) is generic and arises in many physical systems of interest, leading to various forms of solutions $s(x, t)$. (We show examples for different sampled operators in figure 3.) Several methods exist for modeling such PDEs but they require knowledge of the underlying parameters (δ, ν, k) and often impose constraints on the evaluation point as well as expansive time-marching schemes to recover solutions. Here instead, we assume no *a priori* knowledge of the solution and directly regress the operator behavior from the example set \mathcal{E}_O .

Baselines and evaluation We trained our neural regression model on $N_{train} = 500$ different operators $\mathcal{O}_{(\delta, \nu, k, 1)}$ with $t = 1$ fixed and varying number of examples $n \in [20, 100]$ each evaluated at 100 equally spaced points $(x_k)_{k \in [0, 100]}$ on the domain $[0, 1]$. We tested on a set of $N_{test} = 500$ new operators with new diffusion, advection, and reaction

METHOD	RMSE	TIME (s)	GFLOPS
FNO	$2.96e^{-4}$	$1.72e^2$	$1.68e^2$
DEEPONET	$2.02e^{-2}$	$7.85e^1$	$1.54e^2$
TRANSDUCER	$2.39e^{-4}$	$3.10e^{-3}$	$1.06e^{-1}$

Table 1. Mean performance and compute cost of neural operator regression over 50 unseen operators with $n = 50$ examples. Note that DeepONet and FNO are optimized from scratch while the *Transducer* has been pre-trained. GFLOPs represent the total number of floating point (giga-)operations for performing regression.

parameters as well as initial states v . We compared our method with standard machine learning algorithms as well as inductive neural operator approximators. First, we applied standard finite-dimensional regression methods to the discretized problems: $(\mathcal{O}_i(v(x_k))) = u(x_k)_{i,k}$. We apply K -nearest-neighbors (Fix & Hodges, 1989), decision trees (Quinlan, 1986) and kernelized Ridge regression with radial basis kernel (Hastie et al., 2009). Second, we tried to fit two neural-based operators with gradient-descent to the small-sized datasets: DeepONet (Lu et al., 2021) and Fourier Neural operator (FNO) (Li et al., 2020a). Note that for most of these approaches, an explicit optimization scheme is required before inference to fit the target operator. On the other hand, after meta-training, the *Transducer* program amounts to a single feedforward pass of the network, which is orders of magnitude faster (Table 1).

Results First, we verified that our model approximates well unseen operators from the test set (table 1). Furthermore, since our model can perform inference for varying input set sizes, we examined the *Transducer* accuracy when varying

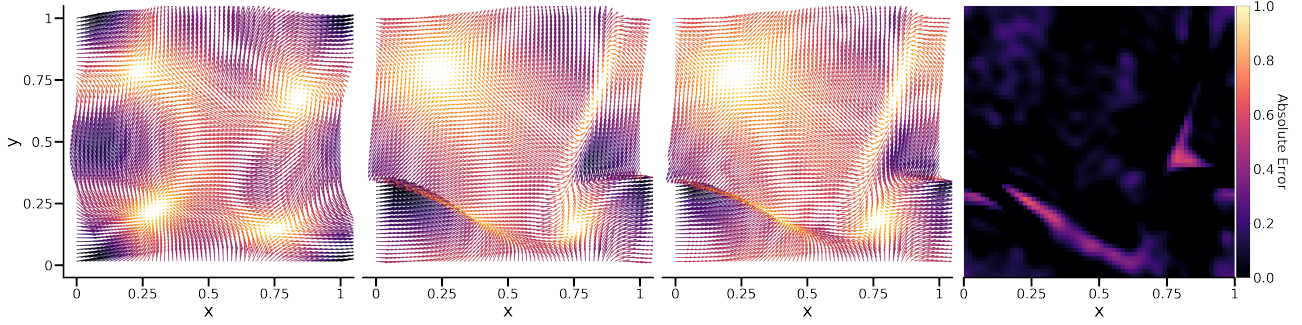


Figure 4. Illustrative example of initial ($t = 0$), target ($t = 10$) and *Transducer* estimation of the vector field $s(\vec{x}, t)$ discretized at resolution 64×64 over the domain $[0, 1]^2$ for the Burger’s equation experiment. The last panel represents absolute error to ground truth.

the number of examples and found that it learns a converging regression program (Figure 3). We noted that our model learns a non-trivial kernel since the linear estimation produced with Nearest Neighbors remains poor even after $1e^3$ examples. Further, our model consistently outperforms other regression approaches to the exception of FNO when enough data is available (> 60). We also found that deeper *Transducer* models with more iterations increase kernel approximation accuracy, with untied weights yielding best performance (figure 3.)

Extrapolation We further tested the *Transducer* ability to regress different operators than those defined in the training set. Specifically, we varied the correlation length (C.L) of the gaussian random fields used to generate functions $\delta(x)$ and $\nu(x)$ in the domain $[0.1, 0.5]^2$ and specified a different target time $t' \neq 1$. We showed that the kernel meta-optimized for a solution at $t = 1$ transfers well to these new regression problems and that regression performance degrades gracefully as the target operators behave further away from the training set. (figure 5)

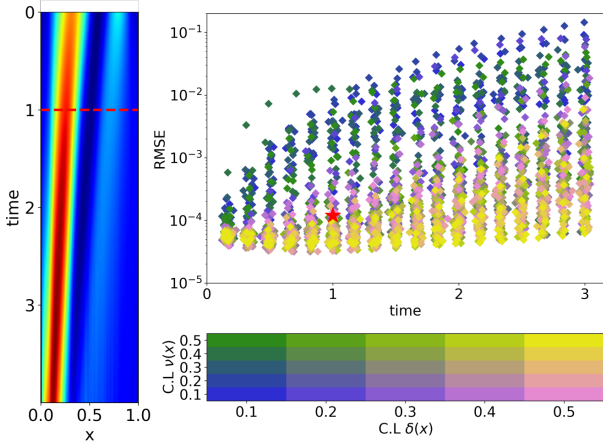


Figure 5. Example of the extrapolated trajectory and Relative Mean Squared Error of the *Transducer* on extrapolation tasks with $n = 100$ examples. Color code corresponds to different correlation lengths used to generate the random functions $\delta(x)$ and $\nu(x)$. Much of the result remains below 1% error despite never being trained on such operators.

Fast and differentiable regression Since our regression model is fully differentiable and orders of magnitude faster than gradient descent, we can execute usually expensive evaluation schemes such as Monte-Carlo Markov Chain to carry out inverse problems, or compute gradients to perform PDE-constrained optimization or even bootstrapping of the regression example set. We leave the full exploration of these applications for future work.

5.2. Burger’s equation in 2D

RMSE	T=1S	T=5S	T=10S
TRANSDUCER	$2.2e^{-3}$	$5.9e^{-3}$	$2.1e^{-2}$

Table 2. Relative MSE on Burger’s 2D regression set for different target times averaged over 200 different parameter conditions $\nu \in [0.1, 0.5]$ and conditioned with 100 examples

We further show that our regression method can fit operators of vector-valued functions. We examine the problem of predicting 2D vector-fields defined as a solution of a two-dimensional Burger’s equation with periodic spatial boundary condition on the domain $\Omega = [0, 1]^2 \times [0, 10]$:

$$\partial_t s(\vec{v}, t) = \underbrace{\nu \Delta_v \cdot s(\vec{v}, t)}_{\text{diffusion}} - \underbrace{s(\vec{v}, t) \nabla_x s(\vec{v}, t)}_{\text{advection}} \quad (12)$$

Here, we condition our model with operators of the form, $v(\vec{x}) = s(\vec{x}, t)$, $u(\vec{x}) = s(\vec{x}, t')$, $s \sim E(\nu)$ such that our model can regress the evolution of the vector field \vec{v} starting at any time, with arbitrary temporal increment $t' - t \leq 10$ seconds and varying diffusion coefficient $\nu \in [0.1, 0.5]$. We show in figure 4 and table 2 that our model is able to fit new instances of this problem with unseen parameters ν .

5.3. Climate modeling

Robust and precise modeling of climate variables is difficult because models need to account for seasonal variables and adapt their prediction to drifting parameters. Even with a globally large amount of available data, the precise operator

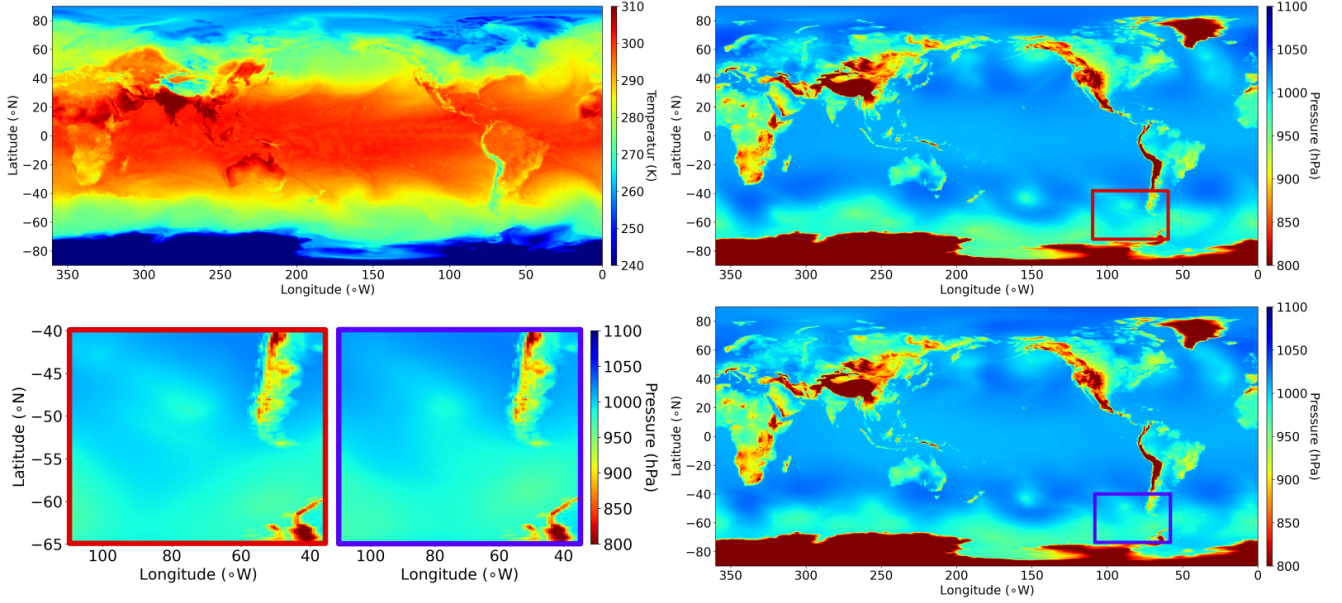


Figure 6. Up - Illustrative examples of 720×720 temperature (left) and pressure (right) fields of the ERA5 dataset. Bottom - Estimated pressure field from conditioning the *Transducer* with 15 days data dating 1 week before the target date. Insets show recovered details of the *Transducer* estimation (blue) compared with ground truth (red).

mapping variables of interest might change over time or be affected by the unobserved phenomenon. Hence, in order to fully exploit the potential of data-driven methods, being able to capture variations in how variables interact might greatly help prediction performance even under operator fluctuation and on data drifting away from the training distribution. One advantage of our approach is the ability to select the data that is most relevant with respect to a certain prediction task and subsequently adapt the model response. In order to illustrate the applicability and scalability of deep transductive learning, we considered the problem of predicting the Earth’s surface air pressure solely from the Earth’s surface air temperature at a high resolution. Data is taken from the ERA5 reanalysis (Hersbach et al., 2020) publicly made available by the ECMWF, which consists of hourly high-resolution estimates of multiple atmospheric variables from 1979 to the current day. We model pressure estimate on a 720×720 grid, resulting in a spatial resolution of $0.25^\circ \times 0.5^\circ$, allowing us to capture small features such as local dynamics and geographic relief. Similar to (Pathak et al., 2022), we modify a ViT backbone to incorporate a kernel transduction layer before every patch attention and compare our model to an unmodified ViT baseline with a matching number of parameters. We additionally compare with a fully transductive Nearest Neighbors approach. In Figure 6 and Table 3, we present results obtained on training a Transducer with data from 2010 to 2014 and testing it on data from 2016 to 2019. We trained our model by predicting 5 random days sampled from random 20-day windows and present two test configurations: We either condition the *Transducer* with a window centered at the

METHOD	LWMSE (hPa)	TIME (s)
NEAREST-NEIGHBORS	67.326	5.915
ViT	32.826	0.053
TRANSDUCER - (P.Y)	25.293	0.192
TRANSDUCER - (P.W)	22.718	0.192

Table 3. Latitude-weighted mean-square error (in hectopascals) and inference time for the surface pressure prediction task.

previous year’s same date (P.Y), or with a 15 days window lagging by a week (P.W). (see SI for details). Both cases outperform transductive and inductive baselines with fast inference time, confirming that our model can scale to large problems.

6. Discussion

We proposed a novel transductive regression model combining kernel principles and neural networks. We grounded our model on the theory of Reproducing Kernel Banach Spaces and applied it to perform operator regression between function spaces. We showcased several instances where it outperformed previous approaches at a lower computational cost. Our approach holds the potential to yield flexible tools for modeling physical systems. However, one limitation is that it relies on meta-training of the model which requires collecting a sufficiently diverse meta-dataset to explore the kernel space. In future work, we plan to investigate methods such as synthetic augmentation to reduce meta-training costs.

References

- Aggarwal, C. C., Hinneburg, A., and Keim, D. A. On the surprising behavior of distance metrics in high dimensional space. In *International conference on database theory*, pp. 420–434. Springer, 2001.
- Ba, J. L., Kiros, J. R., and Hinton, G. E. Layer normalization. *arXiv preprint arXiv:1607.06450*, 2016.
- Bellman, R. Dynamic programming. *Science*, 153(3731): 34–37, 1966.
- Bhattacharya, K., Hosseini, B., Kovachki, N. B., and Stuart, A. M. Model reduction and neural networks for parametric pdes, 2020.
- Boser, B. E., Guyon, I. M., and Vapnik, V. N. A training algorithm for optimal margin classifiers. In *Proceedings of the fifth annual workshop on Computational learning theory*, pp. 144–152, 1992.
- Brown, T., Mann, B., Ryder, N., Subbiah, M., Kaplan, J. D., Dhariwal, P., Neelakantan, A., Shyam, P., Sastry, G., Askell, A., et al. Language models are few-shot learners. *Advances in neural information processing systems*, 33: 1877–1901, 2020.
- Cao, S. Choose a transformer: Fourier or galerkin. *Advances in Neural Information Processing Systems*, 34:24924–24940, 2021.
- Caponnetto, A., Micchelli, C. A., Pontil, M., and Ying, Y. Universal multi-task kernels. *The Journal of Machine Learning Research*, 9:1615–1646, 2008.
- Chen, T. and Chen, H. Universal approximation to nonlinear operators by neural networks with arbitrary activation functions and its application to dynamical systems. *IEEE Transactions on Neural Networks*, 6(4):911–917, 1995.
- Cover, T. and Hart, P. Nearest neighbor pattern classification. *IEEE transactions on information theory*, 13(1):21–27, 1967.
- Dosovitskiy, A., Beyer, L., Kolesnikov, A., Weissenborn, D., Zhai, X., Unterthiner, T., Dehghani, M., Minderer, M., Heigold, G., Gelly, S., Uszkoreit, J., and Hounsby, N. An image is worth 16x16 words: Transformers for image recognition at scale. *ICLR*, 2021.
- Evgeniou, T., Micchelli, C. A., Pontil, M., and Shawe-Taylor, J. Learning multiple tasks with kernel methods. *Journal of machine learning research*, 6(4), 2005.
- Ferraty, F. and Vieu, P. *Nonparametric functional data analysis: theory and practice*, volume 76. Springer, 2006.
- Finn, C., Abbeel, P., and Levine, S. Model-agnostic meta-learning for fast adaptation of deep networks. In Precup, D. and Teh, Y. W. (eds.), *Proceedings of the 34th International Conference on Machine Learning*, volume 70 of *Proceedings of Machine Learning Research*, pp. 1126–1135. PMLR, 06–11 Aug 2017.
- Fix, E. and Hodges, J. L. Discriminatory analysis. non-parametric discrimination: Consistency properties. *International Statistical Review / Revue Internationale de Statistique*, 57(3):238–247, 1989.
- Gamerman, A., Vovk, V., and Vapnik, V. Learning by transduction. In *Proceedings of the Fourteenth conference on Uncertainty in artificial intelligence*, pp. 148–155, 1998.
- Garg, S., Tsipras, D., Liang, P., and Valiant, G. What can transformers learn in-context? a case study of simple function classes, 2022.
- Giles, J. R. Classes of semi-inner-product spaces. *Transactions of the American Mathematical Society*, 129:436–446, 1967.
- Goswami, S., Bora, A., Yu, Y., and Karniadakis, G. E. Physics-informed neural operators. *arXiv preprint arXiv:2207.05748*, 2022.
- Gupta, G., Xiao, X., and Bogdan, P. Multiwavelet-based operator learning for differential equations. *Advances in Neural Information Processing Systems*, 34:24048–24062, 2021.
- Hastie, T., Tibshirani, R., and Friedman, J. The elements of statistical learnin. *Cited on*, 33, 2009.
- Hendrycks, D. and Gimpel, K. Gaussian error linear units (gelus). *arXiv preprint arXiv:1606.08415*, 2016.
- Hersbach, H., Bell, B., Berrisford, P., Hirahara, S., Horányi, A., Muñoz-Sabater, J., Nicolas, J., Peubey, C., Radu, R., Schepers, D., Simmons, A., Soci, C., Abdalla, S., Abellan, X., Balsamo, G., Bechtold, P., Biavati, G., Bidlot, J., Bonavita, M., De Chiara, G., Dahlgren, P., Dee, D., Diamantakis, M., Dragani, R., Flemming, J., Forbes, R., Fuentes, M., Geer, A., Haimberger, L., Healy, S., Hogan, R. J., Hólm, E., Janisková, M., Keeley, S., Laloyaux, P., Lopez, P., Lupu, C., Radnoti, G., de Rosnay, P., Rozum, I., Vamborg, F., Villaume, S., and Thépaut, J.-N. The era5 global reanalysis. *Quarterly Journal of the Royal Meteorological Society*, 146(730):1999–2049, 2020.
- Holl, P., Thuerey, N., and Koltun, V. Learning to control pdes with differentiable physics. In *International Conference on Learning Representations*.

- Jaitly, N., Sussillo, D., Le, Q. V., Vinyals, O., Sutskever, I., and Bengio, S. A neural transducer. *arXiv preprint arXiv:1511.04868*, 2015.
- Jin, P., Lu, L., Tang, Y., and Karniadakis, G. E. Quantifying the generalization error in deep learning in terms of data distribution and neural network smoothness. *Neural Networks*, 130:85–99, 2020.
- Kingma, D. P. and Ba, J. Adam: A method for stochastic optimization. *arXiv preprint arXiv:1412.6980*, 2014.
- Kissas, G., Seidman, J. H., Guilhoto, L. F., Preciado, V. M., Pappas, G. J., and Perdikaris, P. Learning operators with coupled attention. *Journal of Machine Learning Research*, 23(215):1–63, 2022.
- Koehler, D. O. A note on some operator theory in certain semi-inner-product spaces. *Proceedings of the American Mathematical Society*, 30(2):363–366, 1971.
- Laskin, M., Wang, L., Oh, J., Parisotto, E., Spencer, S., Steigerwald, R., Strouse, D., Hansen, S. S., Filos, A., Brooks, E., et al. In-context reinforcement learning with algorithm distillation. In *Deep Reinforcement Learning Workshop NeurIPS 2022*.
- Li, Z., Kovachki, N., Azizzadenesheli, K., Liu, B., Bhattacharya, K., Stuart, A., and Anandkumar, A. Fourier neural operator for parametric partial differential equations. *arXiv preprint arXiv:2010.08895*, 2020a.
- Li, Z., Kovachki, N., Azizzadenesheli, K., Liu, B., Stuart, A., Bhattacharya, K., and Anandkumar, A. Multipole graph neural operator for parametric partial differential equations. In Larochelle, H., Ranzato, M., Hadsell, R., Balcan, M., and Lin, H. (eds.), *Advances in Neural Information Processing Systems*, volume 33, pp. 6755–6766. Curran Associates, Inc., 2020b.
- Lin, R. R., Zhang, H. Z., and Zhang, J. On reproducing kernel banach spaces: Generic definitions and unified framework of constructions. *Acta Mathematica Sinica, English Series*, 38(8):1459–1483, 2022.
- Lu, L., Jin, P., and Karniadakis, G. E. Deeponet: Learning nonlinear operators for identifying differential equations based on the universal approximation theorem of operators. *arXiv preprint arXiv:1910.03193*, 2019.
- Lu, L., Jin, P., Pang, G., Zhang, Z., and Karniadakis, G. E. Learning nonlinear operators via deeponet based on the universal approximation theorem of operators. *Nature Machine Intelligence*, 3(3):218–229, 2021.
- McCloskey, M. and Cohen, N. J. Catastrophic interference in connectionist networks: The sequential learning problem. volume 24 of *Psychology of Learning and Motivation*, pp. 109–165. Academic Press, 1989.
- Mishra, N., Rohaninejad, M., Chen, X., and Abbeel, P. A simple neural attentive meta-learner. In *International Conference on Learning Representations*, 2018.
- Nadaraya, E. A. On estimating regression. *Theory of Probability & Its Applications*, 9(1):141–142, 1964.
- Nelsen, N. H. and Stuart, A. M. The random feature model for input-output maps between banach spaces. *SIAM Journal on Scientific Computing*, 43(5):A3212–A3243, 2021.
- Olsson, C., Elhage, N., Nanda, N., Joseph, N., DasSarma, N., Henighan, T., Mann, B., Askell, A., Bai, Y., Chen, A., et al. In-context learning and induction heads. *arXiv preprint arXiv:2209.11895*, 2022.
- Pathak, J., Subramanian, S., Harrington, P., Raja, S., Chattopadhyay, A., Mardani, M., Kurth, T., Hall, D., Li, Z., Azizzadenesheli, K., Hassanzadeh, P., Kashinath, K., and Anandkumar, A. Fourcastnet: A global data-driven high-resolution weather model using adaptive fourier neural operators, 2022.
- Pedregosa, F., Varoquaux, G., Gramfort, A., Michel, V., Thirion, B., Grisel, O., Blondel, M., Prettenhofer, P., Weiss, R., Dubourg, V., Vanderplas, J., Passos, A., Cournapeau, D., Brucher, M., Perrot, M., and Duchesnay, E. Scikit-learn: Machine learning in Python. *Journal of Machine Learning Research*, 12:2825–2830, 2011.
- Pickering, E., Guth, S., Karniadakis, G. E., and Sapsis, T. P. Discovering and forecasting extreme events via active learning in neural operators. *Nature Computational Science*, 2(12):823–833, 2022.
- Quinlan, J. R. Induction of decision trees. *Machine learning*, 1(1):81–106, 1986.
- Raissi, M., Perdikaris, P., and Karniadakis, G. E. Physics informed deep learning (part i): Data-driven solutions of nonlinear partial differential equations. *arXiv preprint arXiv:1711.10561*, 2017.
- Raissi, M., Perdikaris, P., and Karniadakis, G. E. Physics-informed neural networks: A deep learning framework for solving forward and inverse problems involving nonlinear partial differential equations. *Journal of Computational Physics*, 378:686–707, 2019.
- Ramsauer, H., Schöfl, B., Lehner, J., Seidl, P., Widrich, M., Adler, T., Gruber, L., Holzleitner, M., Pavlović, M., Sandve, G. K., et al. Hopfield networks is all you need. *arXiv preprint arXiv:2008.02217*, 2020.
- Ravi, S. and Larochelle, H. Optimization as a model for few-shot learning. In *ICLR*, 2017.

- Roberts, N. C., Khodak, M., Dao, T., Li, L., Re, C., and Talwalkar, A. Rethinking neural operations for diverse tasks. In Beygelzimer, A., Dauphin, Y., Liang, P., and Vaughan, J. W. (eds.), *Advances in Neural Information Processing Systems*, 2021.
- Santoro, A., Bartunov, S., Botvinick, M., Wierstra, D., and Lillicrap, T. Meta-learning with memory-augmented neural networks. In Balcan, M. F. and Weinberger, K. Q. (eds.), *Proceedings of The 33rd International Conference on Machine Learning*, volume 48 of *Proceedings of Machine Learning Research*, pp. 1842–1850, New York, New York, USA, 20–22 Jun 2016. PMLR.
- Schmidhuber, J., Zhao, J., and Wiering, M. Shifting inductive bias with success-story algorithm, adaptive levin search, and incremental self-improvement. *Machine Learning*, 28, 01 1997.
- Snell, J., Swersky, K., and Zemel, R. Prototypical networks for few-shot learning. In Guyon, I., Luxburg, U. V., Bengio, S., Wallach, H., Fergus, R., Vishwanathan, S., and Garnett, R. (eds.), *Advances in Neural Information Processing Systems*, volume 30. Curran Associates, Inc., 2017a.
- Snell, J., Swersky, K., and Zemel, R. Prototypical networks for few-shot learning. *Advances in neural information processing systems*, 30, 2017b.
- Sung, F., Yang, Y., Zhang, L., Xiang, T., Torr, P. H., and Hospedales, T. M. Learning to compare: Relation network for few-shot learning. In *Proceedings of the IEEE Conference on Computer Vision and Pattern Recognition (CVPR)*, June 2018.
- Szegedy, C., Zaremba, W., Sutskever, I., Bruna, J., Erhan, D., Goodfellow, I., and Fergus, R. Intriguing properties of neural networks. *arXiv preprint arXiv:1312.6199*, 2013.
- Vapnik, V. *The nature of statistical learning theory*. Springer science & business media, 1999.
- Vapnik, V. *Estimation of dependences based on empirical data*. Springer Science & Business Media, 2006.
- Vaswani, A., Shazeer, N., Parmar, N., Uszkoreit, J., Jones, L., Gomez, A. N., Kaiser, L. u., and Polosukhin, I. Attention is all you need. In Guyon, I., Luxburg, U. V., Bengio, S., Wallach, H., Fergus, R., Vishwanathan, S., and Garnett, R. (eds.), *Advances in Neural Information Processing Systems*, volume 30. Curran Associates, Inc., 2017.
- Vilalta, R. and Drissi, Y. A perspective view and survey of meta-learning. *Artif. Intell. Rev.*, 18(2):77–95, oct 2002.
- Vinuesa, R. and Brunton, S. L. Enhancing computational fluid dynamics with machine learning. *Nature Computational Science*, 2(6):358–366, 2022.
- Wang, S., Wang, H., and Perdikaris, P. Learning the solution operator of parametric partial differential equations with physics-informed deepnets. *Science Advances*, 7(40): eabi8605, 2021. doi: 10.1126/sciadv.abi8605.
- Watson, G. S. Smooth regression analysis. *Sankhyā: The Indian Journal of Statistics, Series A*, pp. 359–372, 1964.
- Wen, G., Li, Z., Azizzadenesheli, K., Anandkumar, A., and Benson, S. M. U-fno—an enhanced fourier neural operator-based deep-learning model for multiphase flow. *Advances in Water Resources*, 163:104180, 2022.
- Williams, C. and Rasmussen, C. Gaussian processes for regression. *Advances in neural information processing systems*, 8, 1995.
- Xie, S. M., Raghunathan, A., Liang, P., and Ma, T. An explanation of in-context learning as implicit bayesian inference, 2021.
- Zhang, C., Bengio, S., Hardt, M., Recht, B., and Vinyals, O. Understanding deep learning (still) requires rethinking generalization. *Communications of the ACM*, 64(3):107–115, 2021.
- Zhang, H. Vector-valued reproducing kernel banach spaces with applications to multi-task learning. *Journal of Complexity*, 29(2):195–215, 2013.

Supplementary material : Learning Functional Transduction

A. Details on model hyperparameters and architecture

Discretization – As mentioned in the main text, in order to manipulate functional data, we apply our model on the Fourier transforms of the considered input and output functions and transform its output back to form estimate at arbitrary resolution. We specifically apply our model on the d -dimensional finite vector formed by the first modes of the Fourier transform, and discarding the rest of the function spectrum. For experiments with 2D fields, we describe more precisely in section B.2 how we combine the 2D FFT with our model.

Kernel definition – In order to reduce the number of trainable parameters per layer we split the linear projections defined in the kernel formulation κ_θ into different concatenated "heads" similarly to the Transformer (Vaswani et al., 2017). We also tested a different kernel definition with a radial basis function $f(\mathbf{v}, \mathbf{v}') = \exp(\alpha^{-1} \|\mathbf{v} - \mathbf{v}'\|)$ replacing the dot product-cosine similarity of the key-query attention, yielding similar result in the ADR experiment at an equal compute cost. For coherence, we present all our results with the original kernel definition.

Feedforward network definition For F_θ^ℓ and G_θ^ℓ , we also directly use the Transformer feedforward network architecture defined as one layer perceptron with GeLU activation and Layer normalization (Ba et al., 2016) and did not performed architectural search on this part of the network.

ViT modification – In order to tackle the high-resolution climate modeling experiment, we take inspiration from Pathak et al. (2022), which combines neural operators with the patch splitting method of Vision Transformer (ViT) (Dosovitskiy et al., 2021). Specifically, we split input and output functions into patches of size 40×40 . Since both models operations preserves dimensionality, we interleaves *Transducer* layers that apply kernel transformations κ_θ along the batch dimension with ViT layers performing spatial attention on the set of patched output function representations (\mathbf{u}_i). We drop positional encoding but reduce spatial attention to the neighboring patches for each patch position through masking. We compare this bi-attentional model to a vanilla ViT model that learns by induction a single map from temperature \mathcal{V} to pressure \mathcal{U} . We double the depth of this baseline to match to $L = 12$, in order to match number of trainable parameters.

Hyperparameters

EXPERIMENT	DEPTH	MLP DIM	DIM d	#HEADS	HEADS
ADR	1-8	100	50	32	16
BURGER	10	800	800	64	16
CLIMATE	6	512	512	40	16

Table 4. Summary of the architectural hyperparameters used to build the *Transducer* in our three experiments. 'DEPTH' corresponds to network number of layers, 'MLP dim' to the dimensionality of the hidden layer representation in F_θ^ℓ and G_θ^ℓ , d to the dimension of the discrete function representations.

B. Experiments

B.1. Advection-Diffusion-Reaction operators

Data generation – For our experiment, we collect a meta-dataset of $N = 500$ datasets of the advection-diffusion-reaction trajectories on the domain $\Omega = [0, 1] \times [0, 1]$ by integrating the following equations:

$$\forall n \in \llbracket 1, 500 \rrbracket, \quad \partial_t \mathbf{s}(x, t) = \underbrace{\nabla \cdot (\boldsymbol{\delta}_n(x) \nabla_x \mathbf{s}(x, t))}_{\text{diffusion}} + \underbrace{\boldsymbol{\nu}_n(x) \nabla_x \mathbf{s}(x, t)}_{\text{advection}} + \underbrace{\mathbf{k}_n \cdot (\mathbf{s}(x, t))^2}_{\text{reaction}} \quad (13)$$

using a explicit forward Euler method with step-size $1e^{-2}$ and storing all intermediate solutions on a spatial mesh of 100 equally spaced points. Hence, our discretized reference trajectories are of dimensions 100×100 . For each operator \mathcal{O}_n we

generate spatially varying diffusion and advection coefficients as random function $\delta_n(x) : [0, 1] \mapsto \mathbb{R}$ and $\nu_n(x) : [0, 1] \mapsto \mathbb{R}$ as well as a random scalar reaction coefficient k_n . Defining $\mathcal{G}(0, k_l(x1, x2))$ the one-dimensional zero-mean Gaussian random field with the covariance kernel:

$$k_l(x1, x2) = e^{-\frac{\|x1-x2\|^2}{2l^2}} \quad (14)$$

and length-scale parameter $l = 0.2$, as well as a boundary mask function $m : [0, 1] \mapsto [0, 1], m(x) = 1 - (2x - 1)^{10}$ (to comply with Dirichlet boundary condition and preserve numerical computation stability), we sample $\delta_n(x)$ and $\nu_n(x)$ according to the following equations:

- **diffusion** $\delta_n(x) = 0.01 \times u_n(x)^2 \times m(x)$ where $u_n \sim \mathcal{G}(0, k_{0.2}(x1, x2))$
- **advection** $\nu_n(x) = 0.05 \times y_n(x) \times m(x)$ where $y_n \sim \mathcal{G}(0, k_{0.2}(x1, x2))$
- **reaction** $k_n \sim \mathcal{U}([0, 0.3])$.

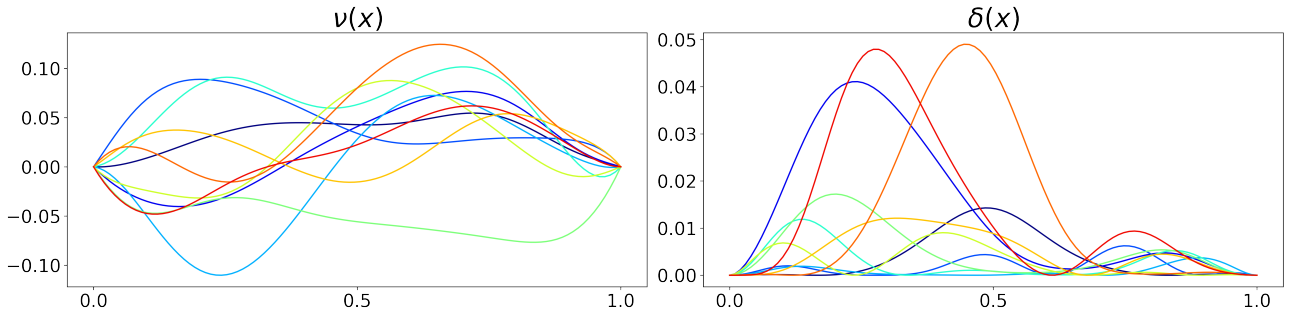


Figure 7. Examples of sampled functions $\delta(x)$ and $\nu(x)$ used to build operators \mathcal{O}_n .

Furthermore, we collect for each dataset $i = 100$ trajectories with each different initial state $s(x, 0) = v_i(x)$, where functions $v_i(x)$ are sampled according to the following:

- **initial state** $v_i(x) = m(x) \times u_i(x)$ where $u_i \sim \mathcal{G}(0, k_{0.2}(x1, x2))$.

For meta-testing, we sample $N = 500$ new datasets of the same generic advection-diffusion-reaction equation with new parameters $\delta_n(x), \nu_n(x), k_n(x)$, for up to 1000 different initial states $v_i(x)$. We present below example of function profiles present in the meta-datasets.

Training – We train Tranducers for 200K gradient steps. At each training step, we randomly draw a single operator \mathcal{O}_n from the meta-training set and isolate the pairs $(v_i, u_i)_{i \leq I} = (s_i(x, 0), s_i(x, 1))_{i \leq I}$ to form the set $\mathcal{E}_{\mathcal{O}_n}$. We sample a "query" subset \mathcal{Q} of $J = 10$ pairs from $\mathcal{E}_{\mathcal{O}_n}$ to be regressed and form the input to our model by concatenating pairs of the query set \mathcal{Q} (with output elements $(u_i)_{i \in \mathcal{Q}}$ set to zero), with a non-overlapping set of $I \in \llbracket 20, 100 \rrbracket$ example elements drawn from $(v_i, u_i)_{i \notin \mathcal{Q}}$. We train our model to minimize the sum of L_2 error between each output function of the set \mathcal{Q} and its corresponding ground truth $u(x) = \mathcal{O}_n(v)(x) = s(x, 1)$ at the 100 discretized positions. We use the Adam optimizer (Kingma & Ba, 2014) with an initial learning rate of $2e - 4$ that is further halved every 50K steps. All the computation operations are coded using the PyTorch library and carried on a single Nvidia Titan Xp GPU with 12GB memory.

Baselines – In order to implement the baseline regression algorithms, we use the scikit-learn library (Pedregosa et al., 2011) for decisions trees, K -nearest neighbours and Ridge regression. We specifically tuned Ridge regression using cross-validation and selected the best-performing 'RBF' kernel with regularisation $\lambda = 1e^{-3}$. For FNO (Li et al., 2020a), we use the official PyTorch implementation provided at dsd and defined for each regression, a 4-layer deep 1-dimensional FNO network with 16 modes and 64-dimensional 1×1 convolutions. For DeepOnet (Lu et al., 2019), we implement our own PyTorch version with 4 hidden layers of 50 hidden units with ReLU activation for the branch and trunk networks.

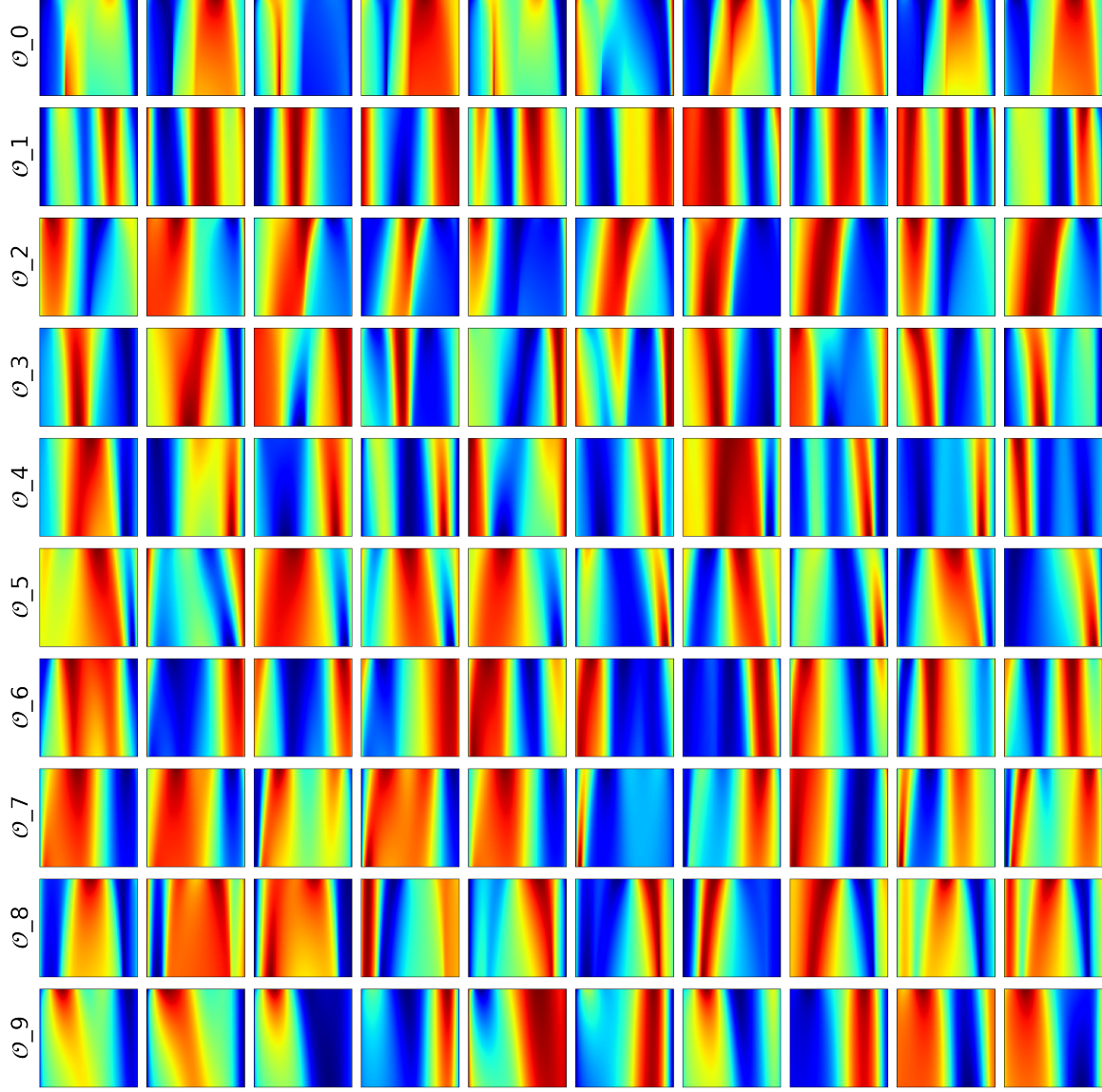


Figure 8. Examples of advection-diffusion-reaction datasets (different operators by row) present in the meta-test set.

Extrapolation experiment – In this task, we modify the generative process of the considered operators by changing the length-scale parameter l used to produce functions $\delta(x)$ and $\nu(x)$, as well as the target time t used to define the operator output.

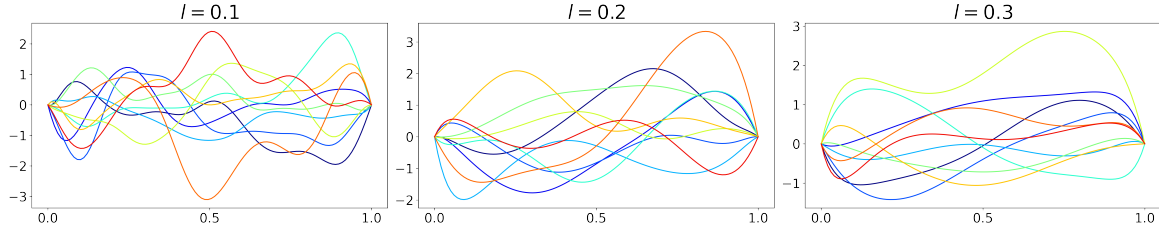


Figure 9. Examples of the spatial function sampled with varying length scale parameter $l \in [0.1, 0.2, 0.3]$

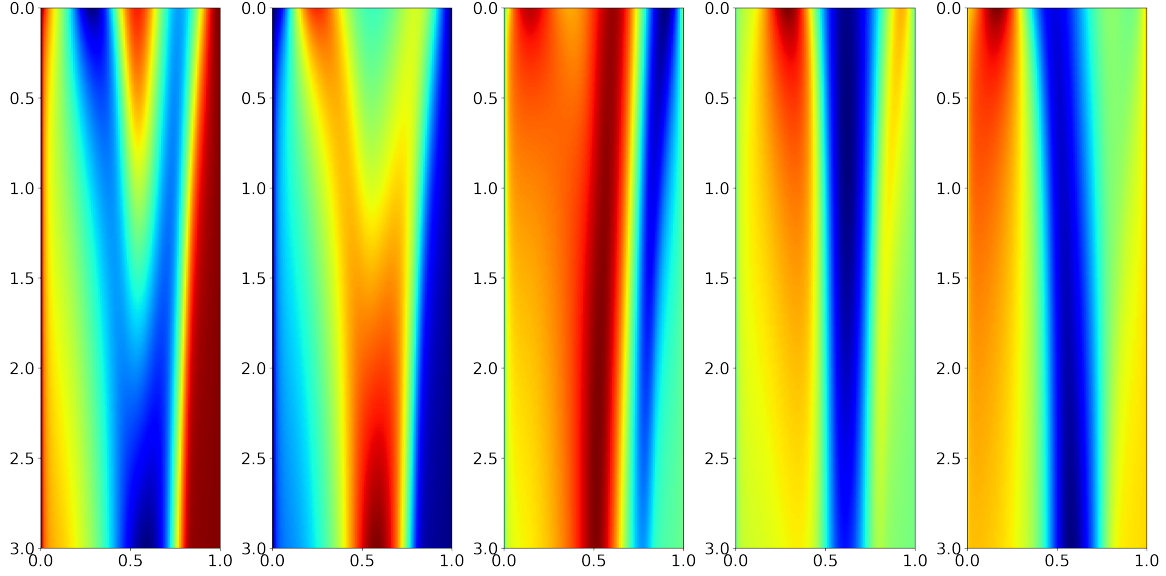


Figure 10. Examples of ADR state evolution forming a set of operators with the same generative parameters but time t allowed to vary in $[0, 3]$

B.2. Burger’s equation

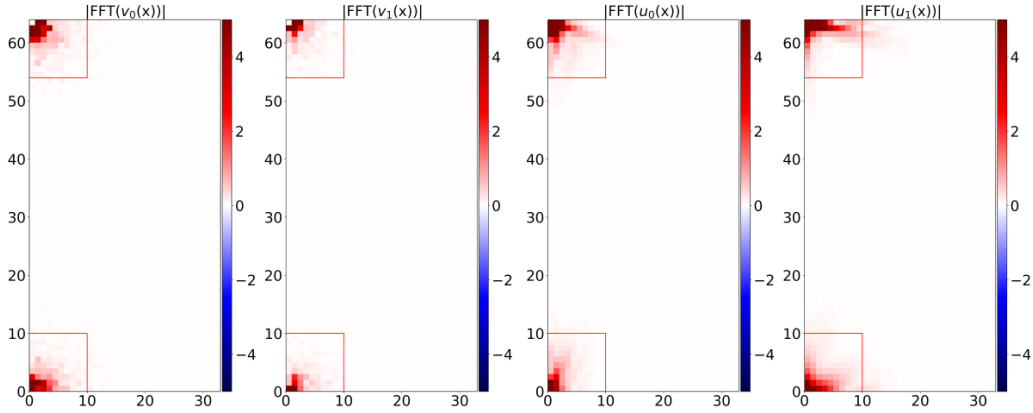


Figure 11. Magnitude of the complex coefficients of the Fourier transform of an exemple pair of input and output functions $(v(\vec{x}), u(\vec{x}))$ in the two coordinates dimension. For every pair, the majority of the signal lies in the two the red quadrants.

Generation – In order to produce the meta-datasets of our second experiment, we use the Φ Flow library (Holl et al.) that allows for batched and differentiable simulations of fluid dynamics and available at <https://github.com/tum-pbs/PhiFlow>. Following the same methodology as experiment 1, we generate batches of the state evolution of random functions $(v_i) : \mathbb{R}^2 \mapsto \mathbb{R}^2$ defined on the domain $\Omega = [0, 1]^2$ at a resolution of 64×64 through different parametrization of equation (4). We form a meta training set of 200 operator datasets for different parameters $\nu \in [0.1, 0.5]$ each of cardinality $I = 100$, and meta testing set of 200 different operator datasets with the same cardinality. Here, we consider vector fields input functions $v(\vec{x})$ whose coordinates $(v_1(\vec{x}), v_2(\vec{x}))$ are drawn each from a two-dimensional zero-mean Gaussian random fields with uniform exponential covariance function and correlation length $l = 0.125$.

Discrete Fourier representation – Since we are dealing with high-dimensional inputs, we perform kernel regression on the 2D fast Fourier transforms of our model. To reduce further dimensionality, since the FFT of a real signals is Hermitian-symmetric, we pass as input to our model only the flattened 10×10 upper and lower quadrants of the Fourier transform coefficients, since we verified that those are sufficient to reconstruct the signal at relative error level of $1e - 5$.

(We present examples of the 2D FFT of our signal.) After regression, we reconstruct our model estimate in the spatial domain at the desired 64×64 resolution and train for the L_2 distance against ground truth.

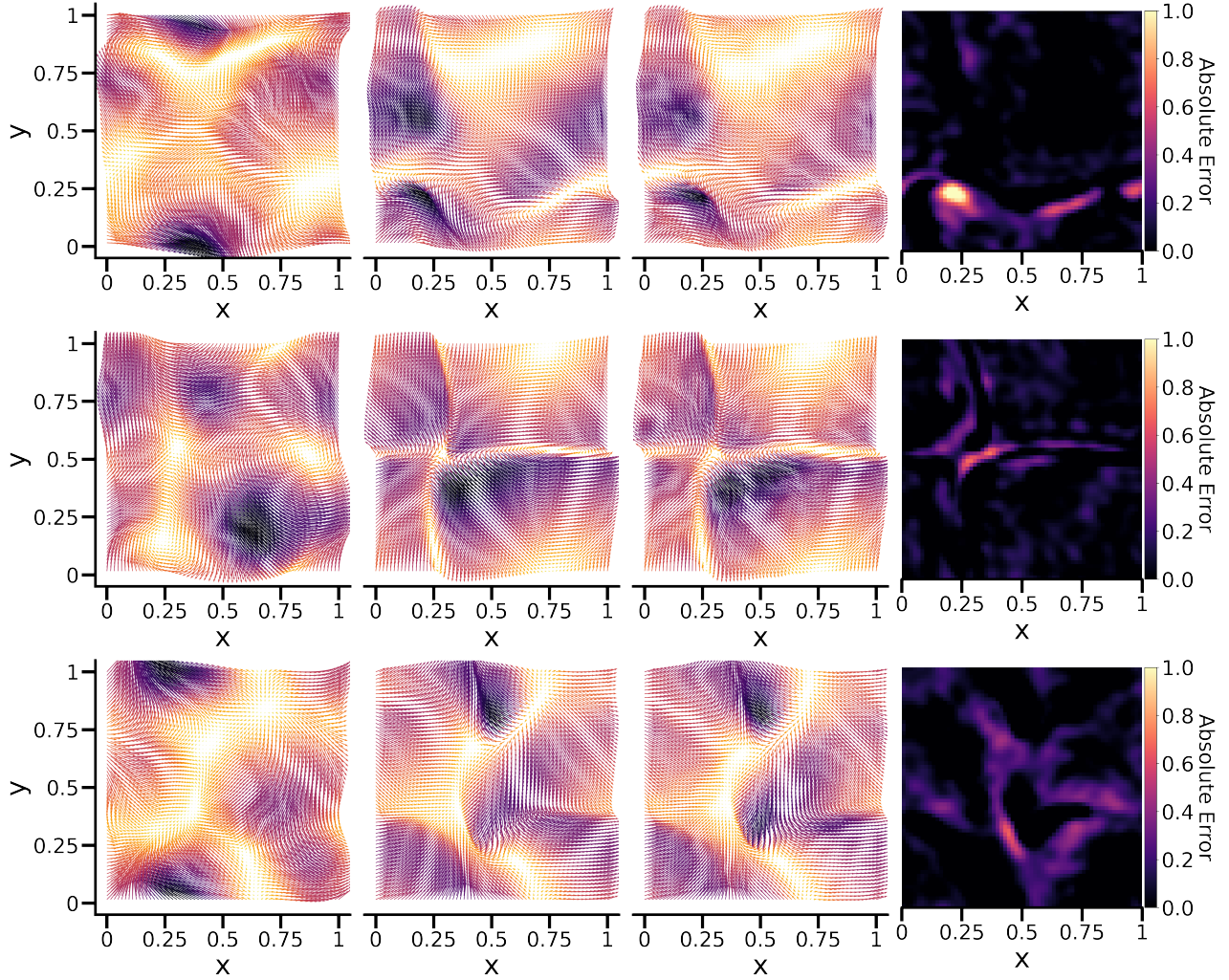


Figure 12. Illustrative examples of initial ($t = 0$), target ($t = 10$) and *Transducer* estimation of the vector field $s(\vec{x}, t)$ discretized at resolution 64×64 over the domain $[0, 1]^2$ for the Burger’s equation experiment. The last panel represents absolute error compared to ground truth.

B.3. Climate modeling

Data – We take our data from ERA5 reanalysis (Hersbach et al., 2020), that is freely available on the Copernicus <https://cds.climate.copernicus.eu/cdsapp#!/dataset/reanalysis-era5-land?tab=overview>. Surface and temperature pressure are re-gridded from a Gaussian grid to a regular Euclidean grid using the standard interpolation scheme provided by the Copernicus Climate Data Store (CDS) to form 2D fields that we further interpolate in the longitude dimension to obtain images of size 720×720 . Although the ERA5 possess hourly estimates, we subsample the dataset by considering only measurement at 12:00am UTC every day.

Training We train our model with learning rate $\lambda = 1e^{-4}$ halved every 50K steps until 200K steps. As mentioned in the main text, we trained our model to predict 5 days randomly sampled from a 20-day window and do not explore larger settings due to GPU memory constraints.